RADAR BACKSCATTER MEASUREMENT ACCURACY FOR SPACEBORNE SCANNING PENCIL-BEAM SCATTEROMETERS

David G. Long

ABSTRACT

A radar scatterometer transmits a series of RF pulses and measures the total-power (energy) of the backscattered signal. Measurements of the backscattered energy from the ocean's surface can be used to infer the near-surface wind vector [7]. Accurate backscatter energy measurements are required to insure accurate wind estimates. Unfortunately, the signal measurement is noisy so a separate measurement of the noise-only total-power is subtracted from the signal measurement to estimate the echo signal energy. A common metric for evaluating the accuracy of the scatterometer energy measurement is the normalized signal variance, termed K_p. In designing a scatterometer tradeoffs in design parameters are made to minimize K_p.

Spaceborne scatterometers have traditionally been based on fan-beam antennas and CW modulation for which expressions for K_p exist. Advanced pencil-beam scatterometers, such as SeaWinds currently being developed by NASA use modulated Signals so that new K_p expressions are required. This paper outlines the derivation of the generalized K_p expression. While very complicated in its exact form, with a simplified geometry the K_p expression can be related to the radar ambiguity function. The resulting analysis yields insights into the tradeoffs inherent in a scatterometer design and permits analytic tradeoffs in system performance.

KEY WORDS

Scatterometry, Measurement Accuracy, SeaWinds

1. INTRODUCTION

Spaceborne wind scatterometers are an important element in future remote sensing systems because of their proven ability to make all-weather measurements of vector winds over the ocean [7]. Wind scatterometry is an indirect technique in which the wind is inferred from measurements of the normalized radar backscatter coefficient (σ^o) using a geophysical model function. The scatterometer transmits a series of RF pulses and measures the energy of the backscattered signal which is corrupted by

noise. A separate measurement of the noise-only energy is subtracted from this measurement to yield the return signal energy. Using the well-known radar equation [8] and the measurement geometry, the backscattered energy measurements are converted into σ^o measurements. Multiple measurements of σ^o from different azimuth and/or incidence angles are used to infer the wind direction. Naderi et al. [7] provide a recent review of scatterometry with emphasis on the NSCAT instrument. NSCAT is an example of a fan-beam Doppler scatterometer. Such systems require large antennas and complicated onboard processors. Scanning pencilbeam scatterometers offer an alternative design concept which can result in smaller, lighter instruments with simpler field-of-view requirements [5, 6]. (Comparisons of fan-beam and pencil-beam scatterometers are contained in [3] and [6].)

A key design goal for scatterometers is to optimize the al measurement accuracy within the design constraints. A common metric for evaluating the accuracy of the σ^o measurement is the so-called K_p parameter [2]. K_p is the normalized standard deviation of σ^o measurement,

$$K_p = \frac{\sqrt{Var\{\sigma^o_{meas}\}}}{\sigma^o}. \tag{1}$$

Expressions for K_p for Doppler fan-beam scatterometers have previously been derived [1, 2]. These expressions are appropriate only for an interrupted-CW transmit signal and a more general expression for a modulated transmit signal is required for analyzing the performance of a pencil-beam scatterometer.

In this paper the derivation of a generalized K_p expression for pencil beam scatterometers is outlined. Beginning with an expression for the return echo, the method for estimating the signal energy is discussed. The K_p expression is related to the radar ambiguity function for a simplified measurement geometry. This enables tradeoffs in the choice of modulation function.

2. RETURN ECHO MODELING

The transmitted radar pulse is $\sqrt{E_t}\, a(t) \exp j\omega_c t$ where t is time, E_t is the transmitted energy per pulse, $\omega_c = 2\pi f_c$, where f_c is the carrier frequency, and $a(t)$ is the carrier modulation function. The pulse length is T_p. The complex modulation function $a(t)$ is normalized to have unit energy and is defined as $a(t) = 0$ for $t < 0$ and $t > T_p$.

The radar echo $\xi_s(t)$ from a large spatially distributed target such as the ocean can be modeled as the superposition of the echo from a very large number of point targets. For a typical spaceborne scatterometer operating at microwave frequencies, the superposition can be expressed as an area integral [8]. For our application we express

the area integral in terms of the Doppler shift and slant range (see Fig. 1). At baseband the return echo can be expressed approximately as

$$\xi_s(t) = \sqrt{X} \int_{r,\omega_d} G(r,\omega_d) a(t-2r/c) e^{-j\omega_d t} e^{j2\omega_c r/c} V_s(r,\omega_d) e^{-j\phi_s(r,\omega_d)} dr d\omega_d. \quad (2)$$

where c is the speed of light, r is the distance (slant range) to the target, T_d is the Doppler shift in radians/sec, and T_c is the carrier frequency in radians/sec. $V_s(r,T_d)\exp\text{-}jN_s(r,T_d)$ is the response function of the target. For a homogeneous target the second moment of target response is

$$E[|V_s(r,\omega_d) e^{-j\phi_s(r,\omega_d)}|^2] = A_r(r,\omega_d)\sigma^o \quad (3)$$

where A_r is the area of the differential element over which the integration is performed. Because of the short correlation length of the surface, V_s and N_s are independent for each differential element. F^o is a function of the wind blowing over the ocean's surface. The radar equation parameter X in Eq. (2) is defined as $X = E_t G_0^2 \delta^2 A_c (4\pi)^{-3} \bar{r}^{-4}$ where $\bar{r}$ is the mean value of of the slant range, δ is the radar wavelength, G_0 is the antenna gain in the direction of the target, and A_c is the effective cell area defined as

$$A_c = \frac{1}{G_0} \int_{r,\omega_d} G(r,\omega_d) A_r(r,\omega_d) dr d\omega_d. \quad (4)$$

For later use we define the weihhted modulation correlation function $K_a(t)$ as

$$K_a(t) = \frac{1}{G_0 A_c} \int_{r,\omega_d} |a(t-2r/c)|^2 G(r,\omega_d) A_r(r,\omega_d) dr d\omega_d, \quad (5)$$

where G_0 is the peak antenna gain over the footprint and the two-dimensional weighted modulation cross-correlation function $J_a(t,J)$ as

$$J_a(t,\tau) = \frac{1}{G_0^2 A_c^2} \int\cdots\int a(t-2r/c) a^*(\tau-2r/c) a^*(t-2r'/c) a(\tau-2r'/c) \cdot G(r,\omega_d) G(r',\omega_d') A_r(r,\omega_d) A_r(r',\omega_d') e^{-j(\omega_d-\omega_d')(t-\tau)} dr d\omega_d dr' d\omega_d'. \quad (6)$$

Finally the weighted time correlation function $L_a(t,J)$ is defined as

$$L_a(t,\tau) = \frac{1}{G A_c} \int_{r,\omega_d} a(t-2r/c) a^*(\tau-2r/c) e^{-j\omega_d(t-\tau)} G(r,\omega_d) A_r(r,\omega_d) dr d\omega_d. \quad (7)$$

2. ENERGY ESTIMATION

Ultimately, we want to estimate the surface F^o from which the wind will be inferred. The F^o estimate is obtained by processing the received echo. Unfortunately, the return echo

is corrupted by additive thermal noise. The received radar signal $\xi_{sn}(t)$ consists of the return echo with additive noise v(t) due to thermal noise in the receiver and the communication channel, i.e., $\xi_{sn}(t) = \xi_s(t) + v(t)$. The downconverted return echo $\xi_s(t)$ (signal) and noise v(t) are assumed to be independent and that the noise is a real white process with a power spectral density of $n_0/2$ over the measurement bandwidth. The signal+noise measurement bandwidth is B_r. The noise-only measurement is made over the bandwidth B_n. (Filters are assumed to be ideal.)

To estimate F^o a measurement of the signal is made by subtracting a "noise-only" measurement from the signal+noise measurement. The noise-only and signal+noise may be made separately (as done by NSCAT) or they may be made simultaneously (planned for SeaWinds). When the measurements are made simultaneously, optimum performance dictates that the bandwidths be distinct (refer to Fig. 1(a)). This results in independent signal+noise and noise-only measurements. However, when the signal+noise and noise-only bandwidths overlap (refer to Fig. 1(b)), the measurements are correlated and the effective K_p is increased. In any case, F^o is inferred from the estimated signal energy. Accurately estimating the signal energy is thus essential to accurately determining F^o. The accuracy of the estimate is quantified by K_p.

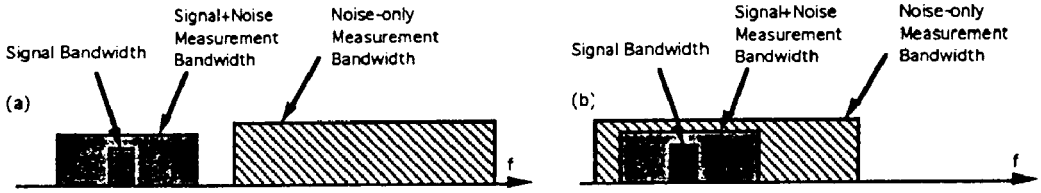

Figure 1: Two cases for simultaneous Signal+Noise and Noise-only measurements. (a) Disjoint measurement bandwidths. Measurements are independent and noise-only measurement bandwidth contains no signal. (b) noise-only measurement bandwidth includes echo signal.

2.1 F^o Estimation

To estimate σ^o, measurements of the signal+noise (C_{sn}) and the noise-only (C_{no}) energy are made. A signal energy estimate $\widehat{E_s}$ is formed as a linear combination of C_{sn} and C_{no}, i.e.,

$$\widehat{E_s} = a_1 C_{sn} + b_1 C_{no} \tag{8}$$

where C_{sn}, C_{no}, a_1, and b_1 are described below. The calculated σ^o value is $\widehat{\sigma^o} = \widehat{E_s}/X$. By proper choice of a_1 and b_1, the energy estimate is unbiased, i.e., $E_s = E[\widehat{E_s}]$. Note that $K_p[\widehat{\sigma^o}] = K_p[\widehat{E_s}]$.

2.2 Energy Estimation

While a variety of possible signal processing and estimation techniques can be used to obtain C_{sn} and C_n, these are limited by practical considerations. For example, the time and frequency dispersion in the echo makes a matched filter power detection very complex and unsuited for onboard processing. Instead, a less optimum, though very simple, power detection scheme is employed. (see Fig. 2)

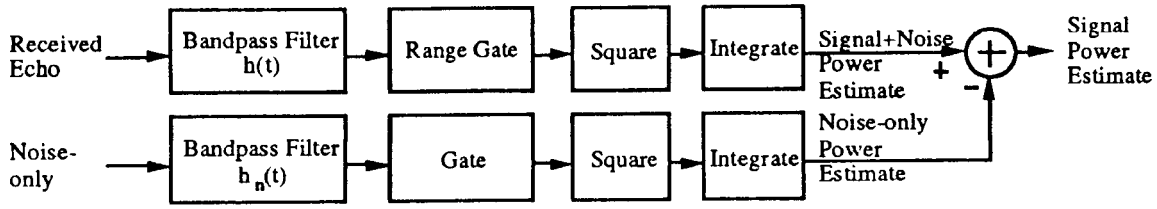

Figure 2: Energy detection scheme

$$C_{sn} = \int_{T_1}^{T_2} |\xi_{sn}(t) * h(t)|^2 dt \qquad \text{Signal+Noise Energy Measurement} \qquad (9)$$

$$C_{no} = \int_{T_3}^{T_4} |\nu(t) * h_n(t)|^2 dt. \qquad \text{Noise-Only Energy Measurement} \qquad (10)$$

If the bandwidth of H(T)is sufficiently wide, the filter does not effect the signal component of $\xi_{sn}(t)$. In this case the signal+noise measurement of Eq. (9) can be expressed as $C_{sn} = C_s + C_n + C_c$ where C_s, is the signal energy C_n is the noise energy, and C_c is the signal and noise cross product, i.e.,

$$C_s = \int_{T_1}^{T_2} |\xi_s(t)|^2 dt \qquad \text{Signal Term} \qquad (11)$$

$$C_n = \int_{T_1}^{T_2} |\nu(t) * h(t)|^2 dt \qquad \text{Noise Term} \qquad (12)$$

$$C_c = \int_{T_1}^{T_2} \{\xi_s(t)[\nu^*(t) * h^*(t)] + \xi_s^*(t)[\nu(t) * h(t)]\} dt \qquad \text{Cross Product Term} \qquad (13)$$

Due to Rayleigh fading the signal energy C_s is "noisy" even without the noise term, i.e., C_{sn}, exhibits variability even when v(t) = 0. The mean signal energy $E|C_s|$ is

$$E[C_s] = X\sigma^o \int_{T_1}^{T_2} K_a(t)dt = \frac{X\sigma^o}{a_1} \triangleq E_s/a_1 \quad \text{with} \quad a_1 = \left[\int_{T_1}^{T_2} K_a(t)dt\right]^{-1}. \qquad (14)$$

The K_p of C_s denoted by K_p', is

$$K_p' = a_1\sqrt{V} \quad \text{with} \quad V = \int_{T_1}^{T_2}\int_{T_1}^{T_2} J_a(t,\tau)dtd\tau. \qquad (15)$$

Assuming ideal low pass filters, [2]

$$E[C_n] = 2B_rT_r\frac{n_0}{2} \triangleq E_n \quad \text{Noise Energy} \tag{16}$$

$$\text{Var}[C_n] = \left(2T_rB_r\frac{n_0}{2}\right)^2 2I(2B_rT_r) \quad \text{Noise Energy -Measurement Variance} \tag{17}$$

$$\text{Var}[C_{no}] = \left(2T_nB_n\frac{n_0}{2}\right)^2 2I(2T_nB_n) \quad \text{Noise-Only Energy Measurement Variance} \tag{18}$$

where $T_r = T_2 - T_1$, $Tn = T_4 - T_3$, and the function I(p) is defined as [2]

$$I(p) = 2\int_0^1 (1-\alpha)\left(\frac{\sin \pi p\alpha}{\pi p\alpha}\right)^2 d\alpha. \tag{19}$$

Note that for large p (corresponding to large time-bandwidth products), $pl(p) \rightarrow 1$. To obtain unbiased measurements the noise-only estimation coefficient b_1 is selected as, $b_1, = a_1 B_rT_r/(B_nT_n)$ so that $E|a_1C_n\text{-}b_1C_{no}| = 0$.

With this background it can be shown (with some effort) that for multiple independent pulses with independent signal+noise and noise-only measurements

$$K_p = \frac{a_1}{\sqrt{N_p}}\left\{V + SU + 2S^2[I(2T_rB_r) + I(2T_nB_n)]\right\}^{1/2} \tag{20}$$

where N_p is the number of independent pulses, U is defined as

$$U = \frac{2}{T_r}\int_{T_1}^{T_2}\int_{T_1}^{T_2} Re[L_a(t,\tau)]\text{sinc}[2B_r(t-\tau)]dtd\tau, \tag{21}$$

and S is the noise-to-signal ratio,

$$S = \frac{1}{E_s}\left(2T_rB_r\frac{n_0}{2}\right). \tag{22}$$

4. K_p VERSUS a(t)

With some rather tedious algebra and assuming that the time-bandwidth product is large it can be shown that Eq. (20) can be approximated by Fisher's [2] K_p equation when the transmit signal is unmodulated, i.e., for interrupted CW operation. Note that V in the general K_p expression [Eq. (20)] corresponds to the variability due to the signal only while U corresponds to the signal cross noise. The S^2 term is not affected by the choice of a(t) (other than by possible need to increase B_r to insure processing of the complete signal bandwidth). With this in mind we will consider just the effect of

the choice of a(t) on the noise-free K_p, $K_p' = a_1\sqrt{V}$. Note that V depends on the measurement geometry.

In order to gain some insight into the effects of different modulation functions on K_p, we assume a simplified geometry and antenna illumination pattern to relate the K_p to the radar ambiguity function, $X_a(J, v)$, defined as

$$X_a(\tau,\nu) = \int_{-\infty}^{\infty} a(t)a^*(t+\tau)e^{j2\pi\nu t}dt. \tag{23}$$

In principle functions defining each term of the K_p equation have to be evaluated separately for each different observation geometry. Because exact expressions are very complicated, a simplified analysis is useful for providing insight into the tradeoff between K_p and a(t). A simplified geometry for the isorange and isodoppler lines is assumed (see Fig. 3) along with a simplified antenna pattern (G = Go within the footprint and zero outside).

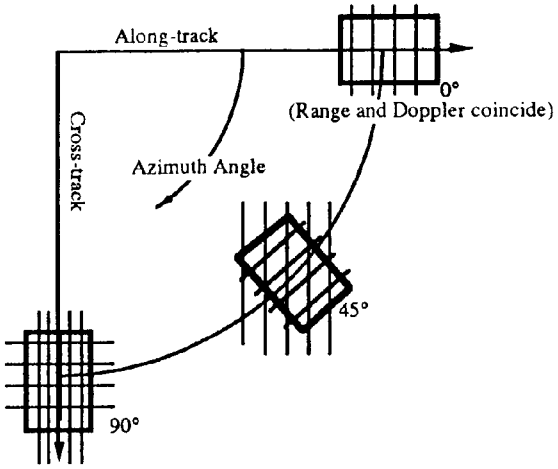

Figure 3: Simplified cell illumination geometry and isolines.

We will consider two cases. Case one corresponds to a 0 ° azimuth angle case while case two corresponds to a 90° azimuth angle. For case two (azimuth angle of 90 °) the integral in Eq. (4) reduces to two integrations in r and T_d with $A_r(r, T_d) = A_c/\Delta r T_D$ where $\Delta r = r_x - r_n$ is the difference between the maximum range r_x and the minimum range r_n over the footprint and $T_D = T_x - T_n$ is the difference between the maximum Doppler T_x and the minimum Doppler T_n over the footprint. For later use we assign $T_c = T_x + T_n$ which the Doppler center frequency and set $\alpha = 2/c$ and Tc = "Δr.

For case one (azimuth angle of 0 °), T_d and r coincide and the integral in Eq. (4) reduces to a line integral. Choosing r as the independent variable, $A_r(r, T_d) = A_c/\Delta r$ with $T_d = \$_r + ($ where $\$ = T_d/\Delta r$ and $(= T_c - T_D/2$ are constants. For the case one (0 ° Azimuth) simplified geometry, a_1^{-1} and V reduce to

$$a_1^{-1} = X_a(0,0)/T_c \text{ and } V = \frac{1}{T_c}\int_{-T_c}^{T_c}(T_c - |y|)\,|X_a(y, \beta y/\alpha)|^2\,dy \tag{24}$$

so that

$$K_p'(\text{case 1}) = \sqrt{\frac{1}{X_a^2(0,0)T_c}\int_{-T_c}^{T_c}(T_c - |y|)\,|X_a(y, \beta y/\alpha)|^2\,dy}. \tag{25}$$

For the case two (90 ° Azimuth) simplified geometry, a_1^{-1} and V reduce to

$$a_1^{-1} = X_a(0,0)/(\omega_D T_c) \text{ and } V = \frac{1}{\omega_D^2 T_c^2}\int_{-T_c}^{T_c}\int_{-\omega_D}^{\omega_D}(T_c - |x|)(\omega_D - |\omega|)\,|X_a(x,\omega)|^2\,dx d\omega \tag{28}$$

with the result that

$$K_p'(\text{case 2}) = \sqrt{\frac{1}{X_a^2(0,0)\omega_D T_c}\int_{-T_c}^{T_c}\int_{-\omega_D}^{\omega_D}(T_c - |x|)(\omega_D - |\omega|)\,|X_a(x,\omega)|^2\,dx d\omega}. \tag{29}$$

4.3 The Relationship of the Ambiguity Function and K_p'

Equations (27) and (25) suggest that the noise-free K_p can be expressed in terms of radar ambiguity function which is a function of the modulation function a(t).K_p' is a weighted function of the volume under (or the area under a diagonal slice of, depending on the geometry case) the ambiguity function. In general, ambiguity functions which are very localized ("thumbtack-like" or concentrated near the origin) result in the smallest K_p' values. Several ambiguity functions are illustrated in Fig. 4. Because the MSK ambiguity function is the most localized, MSK results in a smaller K_p' value. Table 1 summarizes normalized values of K_p' for each modulation scheme. Table I reveals that the choice of the modulation scheme affects the value of K_p' and that K_p' is dependent on the measurement geometry. Comparing the performance of the modulation schemes we find that MSK provides the best performance. Since MSK can be easily generated in hardware, it has been chosen for SeaWinds.

4. TRADEOFFS FOR SeaWinds

The SeaWinds design is used to illustrate the application of these results to improve the scatterometer measurement accuracy. The SeaWinds design is described in detail in [3, 9]. The SeaWinds instrument measures the ocean surface backscatter using two conically scanned pencil beams (see Figure 5). The pattern of measurements on the ground is designed so that each point in the center swath is observed from two to four different azimuth directions. As the antenna rotates, the transmitter pulses first on the inner beam and then on the outer beam. The antenna uses a dual feed to create each beam.

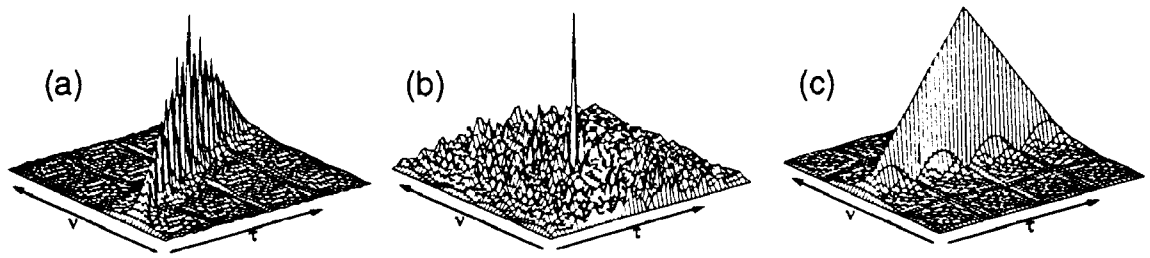

Figure 4: The radar ambugity function (| x(t,τ)|) corresponding to various modulation schemes. (A) LFM (FM chirp). (b) Minimum shift keying (MSK) with a maximal length pseudo-random sequence. © Interrupted CW (ICW).

Modulation	K_p'(case 1)	K_p'(case 2)
ICW	1.0	1.0
LFM	1.0	0.9
MSK	1.0	0.4

Table 1: K_p' for the two simplified geometry cases computed for various transmit signal modulation schemes. The values shown have been normalized by K_p'(case 1: ICW).

In order to keep the Doppler-shifted return echo centered in the narrow signal+noise filter, the Doppler shift imparted by spacecraft motion and the Earth's rotation must be compensated for. To accomplish this, the transmit carrier frequency is varied over ±400 kHz as the antenna rotates so that the return echo appears at the same IF frequency. (Equivalently, the transmit frequency can be kept constant and the IF frequency varied.)

The transmit signal is MSK modulated to a 3 dB bandwidth of B_{msk}. To determine the optimal selection of B_{msk} and hence B_r and B_n for SeaWinds, Eq. (20) was evaluated for SeaWinds design parameters and various signal to noise ratios (corresponding to various wind conditions). For each B_{msk}, the detection bandwidth, B_r was chosen such that $B_r = B_{msk} + 40$ kHz, allowing the detection filter to accommodate the modulation bandwidth as well as an approximately 40 kHz Doppler tracking uncertainty. B_n is chosen to be very large (1 MHz) to minimize the noise contribution to K_p.

K_p increases with SNR. For any given SNR, as B_{msk} is increased K_p first decreases, then increases. Optimum K_p performance for low wind speeds (corresponding to low signal to noise ratios) is achieved for an MSK modulation bandwidth of $B_{msk} = 40$ kHz. This bandwidth can be created by modulating the transmit signal with a 70 kHz maximal length sequence. The required B_r is thus 80 kHz.

5. CONCLUSION

An expression for the measurement K_p for a F^o measurement from a pencil-beam scatterometer has been derived. The general K_p expression includes transmit signal modulation. The radar ambiguity function approach can be useful in making first-order tradeoffs in modulation functions to minimize the noisefree K_p. MSK provides the best overall improvement in the total K_p but the amount of improvement is dependent on the measurement geometry. Using the expression. a modulation bandwidth has been selected for SeaWinds.

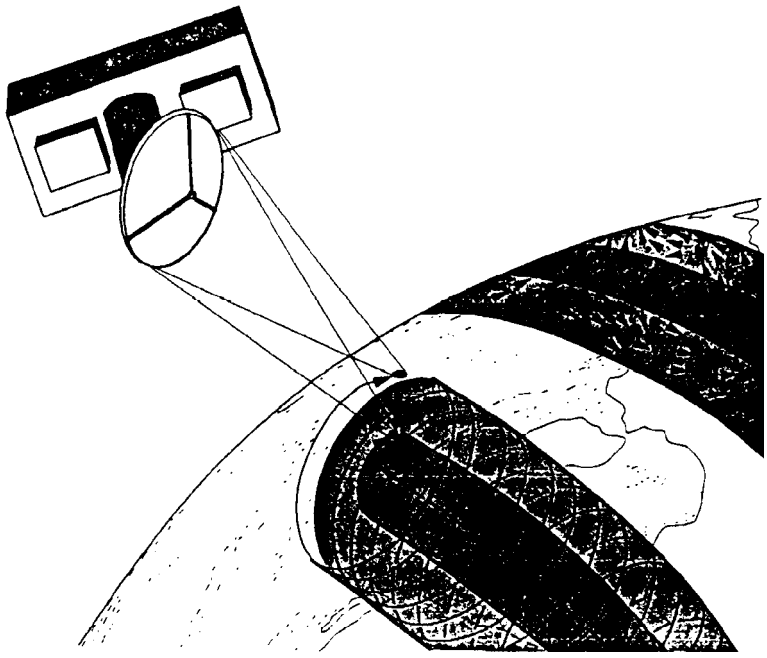

Figure 5: SeaWinds scanning concept. Each beam traces out a helix as the spacecraft moves.

ACKNOWLEDGMENTS

The assistance of M.W. Spencer at the Jet Propulsion Laboratory, California Institute of Technology and T. Oliphant at Brigham Young University is gratefully acknowledged.

References

[1] Chi, C-Y, Long, D.G., and Li, F.K., "Radar Backscatter Measurement Accuracies Using Digital Doppler Processors in Spaceborne Scatterometers," IEEE Trans. Geosci. Rem. Sens. , Vol. GE-24, No.3, May 1986, pp. 426-437.

[2] Fisher, R., "Standard Deviation of Scatterometer Measurements From Space," IEEE Trans. Geosci. Electron. , Vol. GE-10, No. 2, April 1972, pp. 106-113.

[3] Freilich, M.H., Long, D.G., and Spencer, M.W.,"SeaWinds: A Scanning Scatterometer for ADEOS II - Science Overview," Proc. IGARSS'94, Pasadena, California, August 8-12, 1994, pp. 960-963.

[4] Long, D.G., and Spencer, M.W., "Radar Backscatter Measurement Accuracy for Spaceborne Scanning Pencil-Beam Scatterometers " submitted to IEEE Trans. Geosci. Rem. Sens., 1995.

[5] Long, D.G., "ASCAT: A Light-Weight, Low-Cost Scatterometer," in Microwave Instrumentation for Remote Sensing of the Earth , James. C. Shiue, ed., Proc. SPIE 1935, Orlando, Florida, April 13-14, 1993, pp. 28-38.

[6] Long, D.G., Freilich, M.H., Leotta, D.F., and Noon, D.E., "A Scanning Scatterometer for the Eos Polar Platform," Proc. IGARSS'90, Washington, D.C., May 20-24, 1990, pp. 2447-2450.

[7] Naderi, F., Freilich, M.H., and Long, D.G., "Spaceborne Radar Measurement of Wind Velocity Over the Ocean-An Overview of the NSCAT Scatterometer System," Proc. IEEE, Vol. 79, No. 6, June 1991, pp. 850-866.

[8] Ulaby, F.T., Moore, R.K., and Fung, A.K., Microwave Remote Sensing - Active and Passive, Addison-Wesley Publishing Company, Reading, MA, 1981.

[9] Wu, C., Graf, J., Freilich, M., Long. D.G., Spencer, M., Tsai, W., Lisman, D., and Winn, C., "The SeaWinds Scatterometer Instrument," Proc. IGARSS'94, Pasadena, California, August 8-12, 1994, pp. 1511-1515.